The effect of confinement on rock failure behaviour under high-velocity impact

Jing Li[1], Qianbing Zhang[2], Chor Kin Tsang[1], Tong Joo SIA[1].

[1]SMEC Australia, Melbourne, VIC 3008, Australia; email: frank.li@smec.com; ck.tsang@smec.com; tongjoo.sia@smec.com.
[2]Civil Engineering, Monash University, VIC 3800, Australia; email: qianbing.zhang@monash.edu.

ABSTRACT

The result of redistributed quasi-static stress and/or dynamic sources can be serious underground disasters such as rock bursts. Rock failure characteristics are heavily affected by loading rates and confinement. A deep understanding of their roles has practical significance in evaluating the stability and the design of underground engineering. In this study, specimens were first confined under quasi-static uniaxial, biaxial and triaxial pre-stress conditions and then these were impacted by the launch of a high-velocity striker using a triaxial Hopkinson bar system. A high-speed imaging technique was used to record real-time deformation and fracturing processes. The rock dynamic behaviours such as stress-strain behaviours and energy evolutions were quantitatively investigated. The relationship between mechanical properties and fragmentation features was also presented.

Keywords: rock dynamic behaviours, confinement effects, fragmentation, triaxial Hopkinson bar

1 INTRODUCTION

Underground mining and tunnelling excavation significantly change the natural stress field of the surrounding rock mass. Rock will be damaged when the stress exceeds its strength limit. Analysis and prediction of rock failure is one of the key purposes of rock mechanics. Rock damage under quasi-static conditions have been extensively studied from failure criterion, energy evolution, micro-seismicity and so on (Hoek, 1964; Mogi, 1971, Lockner et al. 1991, Niandou et al. 1997, Hazzard and Young, 2000). These research findings have provided important guidance on engineering practices. Rock can also fail suddenly due to various dynamic/seismic loads from fault slip, roof breakage and blasting. Figure 1 shows an example of a coal burst hazard triggered by dynamic sources. Rock failure under dynamic loads has more complex characteristics due to strain rate effects. Numerous experimental studies have been carried out in this regard mainly using a split Hopkinson pressure bar (SHPB) system (Field et al. 2004; Kolsky, 1949). Comprehensive reviews on experimental techniques and mechanical behaviours of rock dynamic tests can be found in Zhang and Zhao (2014).

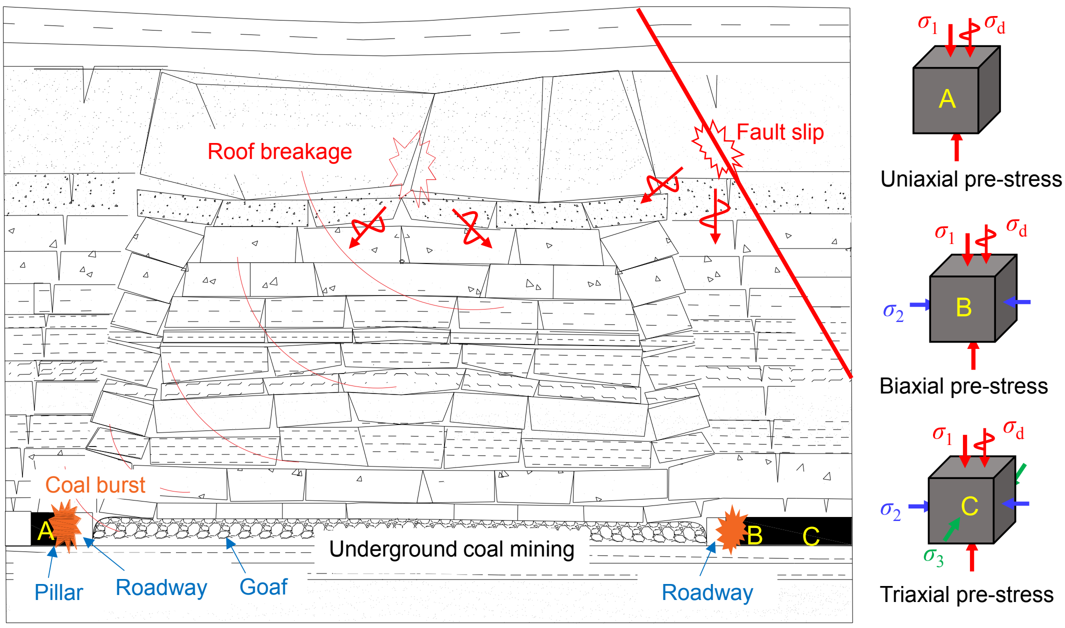

Figure 1: Coal stress states and coal burst hazards in mining. σ_1, σ_2 and σ_3 are maximum, intermediate and minimum principal stress, respectively. σ_d means dynamic loading.

Confinement is one of the most important factors affecting rock behaviour. The SHPB was also further improved so that confinement can be applied on the tested specimens (Christensen et al., 1972; Frew et al. 2010; Li et al. 2008). More recently, triaxial Hopkinson pressure bar was developed aiming to apply biaxial/true-triaxial pre-stresses and dynamic loads (Liu et al. 2019; Zhang et al. 2021; Li et al. 2021). Experimental results showed that improving confinement not only can significantly increase rock bearing capacity, but also change failure patterns. However, there is still a lack of research on dynamic mechanical and fracturing characteristics of rock under the coupled effect of strain rates and confinement. A comprehensive investigation of the coupled static and dynamic loads under different confinement types is of critical knowledge for the prevention of potential hazards and the improvement of underground engineering safety.

In this study, dynamic uniaxial, biaxial and triaxial tests were conducted on rock specimens by using a triaxial Hopkinson bar system, respectively. Real-time rock deformation and fracturing process were captured by high-speed cameras. The relationships among stress-strain response, peak stress, and failure patterns were explored and discussed in detail.

2 EXPERIMENTAL TESTS AND DATA ACQUISITION

Dynamic uniaxial, biaxial and triaxial compressive tests were conducted using a triaxial Hopkinson bar (Tri-HB) system, as shown in Figure 2. In the tests, a cubic specimen was placed in the loading cell where quasi-static confinement can be applied by movements of square steel bars aligned orthogonally in X, Y and Z directions. After the desired confinement was achieved, the dynamic loading was applied by the launch of the striker compressed by the gas gun. When the striker hits the incident bar, a compressive stress wave propagates towards the specimen and a transmission wave is generated in the transmission bar in the X direction. Meanwhile, the wave also propagates in the Y and Z bars. The velocity of the striker bar is measured by a laser-beam velocity measurement system. A detailed introduction to the Tri-HB system is provided in previous publications (Liu et al. 2019; Liu et al. 2020; Zhang et al. 2021). The dynamic stress σ, strain rate $\dot{\varepsilon}$ and strain ε can be obtained from incident, reflected and transmission waves recorded by strain gauges (Kolsky, 1949; Cadoni and Albertini, 2011). The energy carried in these waves can also be further calculated.

In this study, coal specimens with Uniaxial Compressive Strength (UCS) of 27.16 MPa and elastic modulus of 2.17 GPa were prepared for the tests. For the dynamic uniaxial compressive (UC) tests, the specimen was impacted without quasi-static confinement. In the dynamic biaxial compressive (BC) tests, the specimen was subjected to impacting under biaxial quasi-static pre-tress conditions. Biaxial pre-stresses σ_1 =10 MPa and σ_2 = 5 MPa were applied on the specimens in the X and Y directions, respectively. In the dynamic biaxial compressive (TC) tests, the specimen was impacted under triaxial pre-stresses σ_1 = 15 MPa, σ_2 = 10 MPa and σ_3 = 5 MPa in the X, Y and Y directions, respectively. For all the tests, impact was along the X direction.

(a) (b)

Figure 2: Triaxial Hopkinson bar at Monash University (a) and a standard cubic coal specimen placed between bars in the loading cell (b).

3 RESULTS AND DISCUSSION

3.1 Stress-strain responses

Figure 3a-c shows the effect of strain rates on the dynamic stress-strain curves for specimens under uniaxial, biaxial and triaxial pre-stress conditions. Two types of stress-strain curve Class-I and Class-II can be observed according the evolution of strain and stress with loading process. For Class-I stress-strain curves, the dynamic strain continually increases to the peak and then decreases, while dynamic strain keeps increasing during the whole loading process for Class-II types. The strain recovery in the unloading stage of Class-I type prevents further failure of specimens, however continued deformation leads to the specimen failure for Class-II type curves. Experiments indicate that only Class-II type stress-strain curves were exhibited by specimens under uniaxial confinement. This means that specimens were damaged and did not have sufficient bearing capacity under this loading condition. Failure patterns also demonstrate that specimens were shattered into multiple fragments and the degree of fragmentation increased with increasing strain rates as shown in Figure 3a. For specimens under biaxial confinement, stress-strain curves gradually changed from Class-I to Class-II type as strain rate increased. At strain rates of 87.4 s^{-1} and 125.7 s^{-1}, specimens remained macroscopically or partially intact since the applied dynamic loading was insufficient to break specimens. The failure modes correspond to the Class-I stress-strain type, where the strain reduces gradually with the decrease of stress at post-peak stage. Specimens were pulverised into fragments when the strain rate exceeded the 188.4 s^{-1} as shown in Figure 3b. For specimens under triaxial confinements, the stress-strain curves always remained Class-I type when the strain rates increased from 107.5 s^{-1} to 191.2 s^{-1}. Failure patterns also show that specimens were not damaged as shown in Figure 3c. Figure 3d illustrates the relationships among peak stresses, strain rates and confinement. The peak stress exhibits an upward trend with the increasing strain rates under any confinement type. At the same strain rate, increasing restraints can improve specimen bearing capacity. Besides, strain rate sensitivity of peak stresses sees an increasing trend when the confinement type was changed from uniaxial to triaxial conditions.

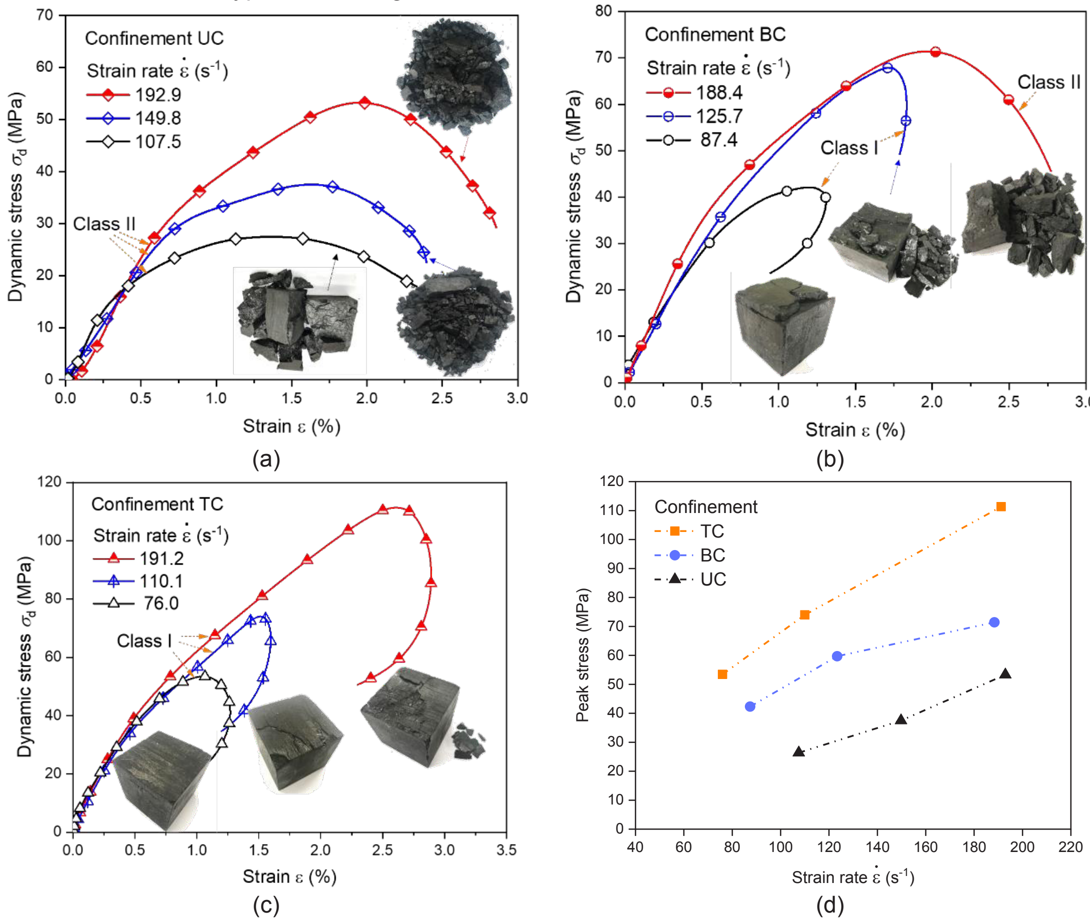

Figure 3: Stress-strain curves (a-c) and peak stresses (d) under the effect of strain rates and confinements.

3.2 Energy evolution

Table 1 compares the high-speed photography of rock dynamic failure process under uniaxial and biaxial confinement. Under UC conditions, the specimen deforms elastically without visible cracks on the surface at the initial loading stage, and several cracks parallel to impact direction emerge with further loading. These tensile cracks are caused by tension perpendicular to the impact direction. As the strain rate increases, more tensile cracks are produced, and the fragmentation degree is further improved. When the specimen is confined under BC conditions, biaxial prestresses cause the splitting failure of exposed surfaces, and flake surface into small fragments.

Table 1: Specimen failure patterns with the influence of strain rates and confinement. The yellow arrow indicates impacting direction.

Confinement	Strain rate/s	High-speed photographs of specimen fracturing processes			
		t = 0 *ms*	0.2 *ms*	1 *ms*	1.7 *ms*
UC	107.5	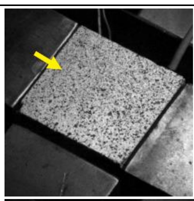	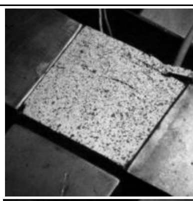	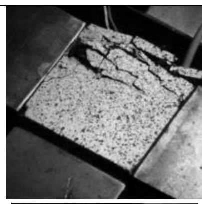	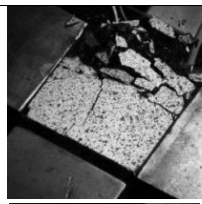
UC	149.8	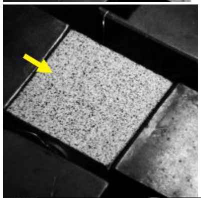	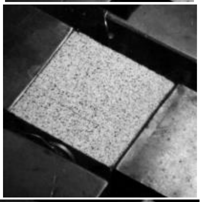	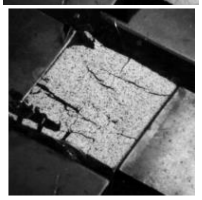	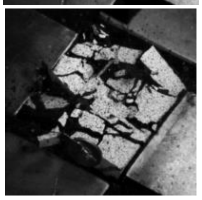
BC	125.7	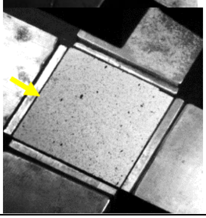	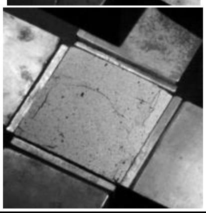	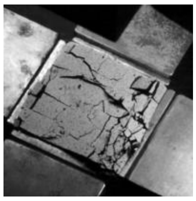	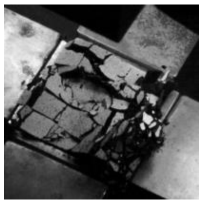

Energy absorption and dissipation are involved in the rock deformation and fracturing process. When the striker hits the incident bar, an incident wave propagates towards the specimen, and meanwhile reflected and transmission waves are generated. The incident, reflected, transmitted waves can be extracted with signals captured by strain gauges attached on the Tri-HB system, and incident (W_{in}), reflected (W_{re}) and transmission (W_{tr}) energies carried by these waves can be calculated accordingly (Liu et al., 2020). Besides, a portion of the input incident energy is absorbed by specimens (W_s) to create fracture surface and micro-cracks. The amount of energy absorbed by rock specimens directly determines the damage severity.

Figure 4 presents the energy evolutions for specimens under uniaxial, biaxial and triaxial confinement at a strain rate of around 190 s^{-1}. For specimens under different pre-stress conditions, the evolution of various energies is similar in the deformation and fracturing stages. The energies increase slowly at the initial dynamic loading stage, while at 100 μs these energies increase sharply and growth rate slows down above 250 μs. Confinement plays a significant role in energy distribution. To achieve the same strain rate, the triaxially confined specimens require the highest input incident energy, while the lowest input energy is found for uniaxially confined specimens.

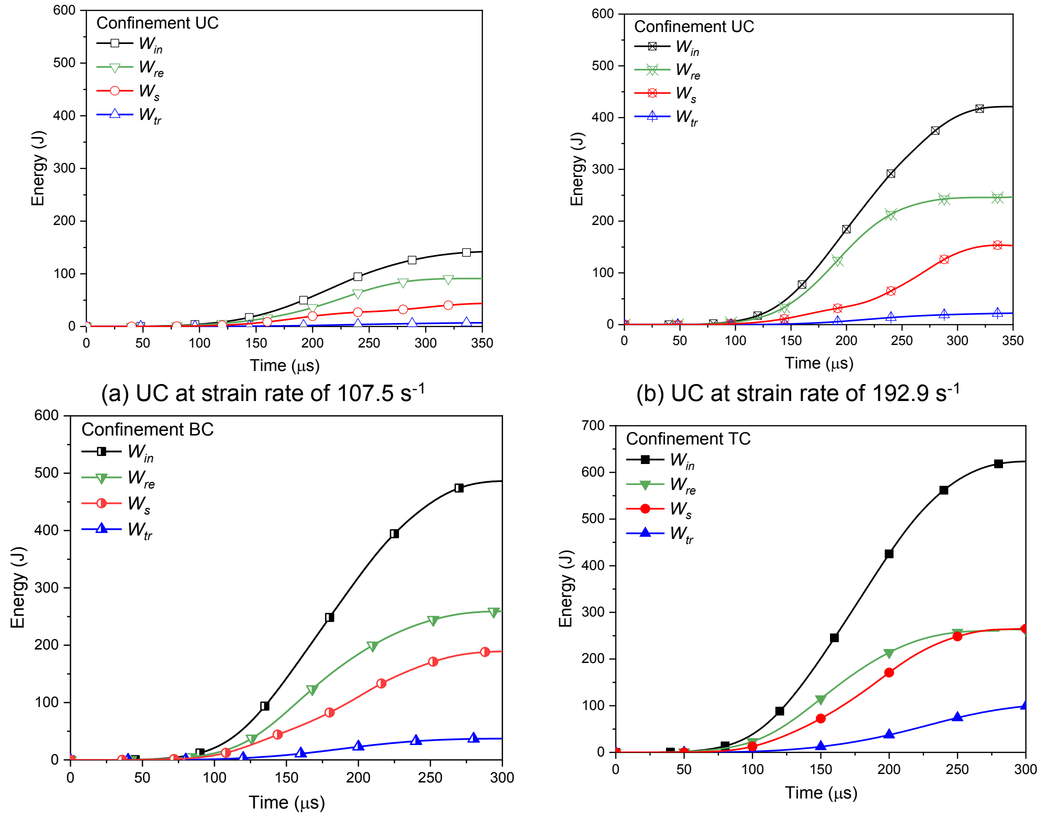

(a) UC at strain rate of 107.5 s^{-1} (b) UC at strain rate of 192.9 s^{-1}

(c) BC at strain rate of 188.4 s^{-1} (d) UC at strain rate of 191.2 s^{-1}

Figure 4: Energy evolutions for specimens under uniaxial, biaxial and triaxial confinements.

Figure 5 shows the effect of confinement type on the absorption energy at high-velocity impacting. Increasing strain rates or the input incident energy can make the specimen absorb more energy and meanwhile increase the fragmentation degree as indicated in Figure 3. At the same strain rate or incident energy, the largest absorption energy is observed when triaxially confined (TC) while the lowest value is found for Uniaxial confinement (UC). The varied energy absorption abilities are caused by difficulties in creating cracks. More energy will be consumed to create cracks with increasing confinement. To achieve the same fragmentation degree, specimens under TC consume the most amount of energy, while the minimum energy consumption is required to achieve the same damage degree for UC. This also offers an explanation why the specimen is failed at the strain rate of 107.5 s^{-1}, while triaxially confined specimens remain intact at a strain rate of 191.2 s^{-1}.

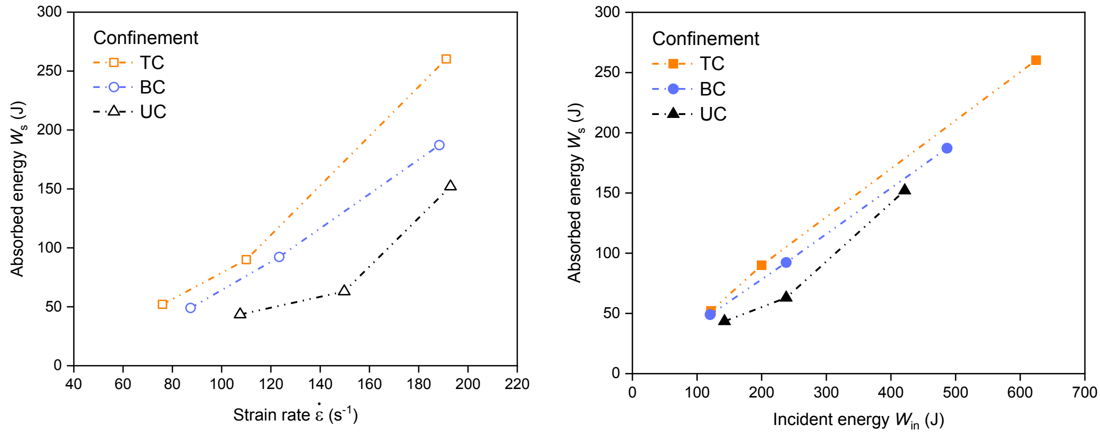

(a) (b)

Figure 5: Correlation between specimen absorbed energy with strain rates (a) and incident energy (b).

4 CONCLUSION

In this study, the effect of strain rate and confinement type on the rock mechanical and fracturing properties was investigated using a triaxial Hopkinson Bar system. Experimental results show that increasing strain rates improve the rock strength but also decrease its integrity. Increasing confinement can significantly reduce the fragmentation degree while increasing the ability of the rock to resist dynamic loads. Energy evolution analysis indicates that as the strain rate increases, more energy is absorbed to generate cracks. At the same strain rate, crack generation requires the minimum absorbed energy for uniaxial confinement, while the highest energy is absorbed in the triaxial case.

5 ACKNOWLEDGEMENTS

This work was financially supported by the Australian Research Council (LE150100058 and DE200101293).

REFERENCES

Cadoni, E., and Albertini, C. (2011). “Modified Hopkinson bar technologies applied to the high strain rate rock tests.” Adv Rock Dyn Appl. 79–104.
Christensen, R., Swanson, S., and Brown, W. (1972). “Split-Hopkinson-bar tests on rock under confining pressure.” Experimental Mechanics 12, 508-513.
Field, J.E., Walley, S.M., Proud, W.G., Goldrein, H.T., and Siviour, C.R. (2004). “Review of experimental techniques for high rate deformation and shock studies.” International Journal of Impact Engineering 30, 725-775.
Frew, D.J., Akers, S.A., Chen, W., and Green, M.L. (2010). “Development of a dynamic triaxial Kolsky bar.” Measurement Science and Technology 21.
Hazzard, J.F., and Young, R.P. (2000). “Simulating acoustic emissions in bonded-particle models of rock.” International journal of rock mechanics and mining sciences 37, 867-872.
Hoek, E. (1964). “Fracture of anisotropic rock.” Journal of the South African Institute of Mining and Metallurgy 64, 501-518.
Kolsky H. (1949). “An investigation of the mechanical properties of materials at very high rates of loading.” Proceedings of the Physical Society. Section B 62, 676-700.
Li, J., Zhao, J., Gong, S.Y., Wang, H.C., Ju, M.H., Du, K., and Zhang, Q.B. (2021). “Mechanical anisotropy of coal under coupled biaxial static and dynamic loads.” International Journal of Rock Mechanics and Mining Sciences, 143, 104807.
Li, X.B., Zhou, Z.L., Lok, T.-S., Hong, L., and Yin, T.B. (2008). “Innovative testing technique of rock subjected to coupled static and dynamic loads.” International Journal of Rock Mechanics and Mining Sciences 45, 739-748.
Liu, K., Zhang, Q.B., Wu, G., Li, J.C., and Zhao, J. (2019). “Dynamic mechanical and fracture behaviour of sandstone under multiaxial loads using a triaxial Hopkinson bar.” Rock Mechanics and Rock Engineering 52, 2175-2195.
Liu, K., Zhao, J., Wu, G., Maksimenko, A., Haque, A., and Zhang Q.B. (2020). “Dynamic strength and failure modes of sandstone under biaxial compression.” International Journal of Rock Mechanics and Mining Sciences 128.
Lockner, D.A., Byerlee, J.D., Kuksenko, V., Ponomarev, A., and Sidorin, A. (1991). “Quasi-static fault growth and shear fracture energy in granite.” Nature 350, 39-42.
Mogi, K. (1971). “Fracture and flow of rocks under high triaxial compression.” Journal of Geophysical Research 76, 1255-1269.
Niandou, H., Shao, J.F., Henry, J.P., and Fourmaintraux, D. (1997). “Laboratory investigation of the mechanical behaviour of Tournemire shale.” International Journal of Rock Mechanics and Mining Sciences 34, 3-16.
Zhang, Q.B., and Zhao, J. (2014). “A Review of Dynamic Experimental Techniques and Mechanical Behaviour of Rock Materials.” Rock Mechanics and Rock Engineering 47, 1411-1478.
Zhang, Q.B., Liu, K., Wu, G., and Zhao, J. (2021). “Dynamic Deformation, Damage, and Fracture in Geomaterials.” Voyiadjis G.Z. (eds) Handbook of Damage Mechanics, 1-44.